The Journal of Clinical Endocrinology & Metabolism, 2025, **00**, 1–11
https://doi.org/10.1210/clinem/dgae899
Advance access publication 2 January 2025
Clinical Research Article

Stimulation of Piezo1 Mechanosensitive Channels Inhibits Adipogenesis in Thyroid Eye Disease

Erika Galgoczi,[1] Istvan Orsos,[1] Zsanett Molnar,[1] Bernadett Ujhelyi,[2] Zita Steiber,[2] Laszlo Szabo,[3] Beatrix Dienes,[3,4] Laszlo Csernoch,[3,4] Endre V. Nagy,[1] and Monika Katko[1]

[1]Division of Endocrinology, Department of Internal Medicine, Faculty of Medicine, University of Debrecen, 4032 Debrecen, Hungary
[2]Department of Ophthalmology, Faculty of Medicine, University of Debrecen, 4032 Debrecen, Hungary
[3]HUN-REN DE Cell Physiology Research Group, Faculty of Medicine, University of Debrecen, 4032 Debrecen, Hungary
[4]Department of Physiology, Faculty of Medicine, University of Debrecen, 4032 Debrecen, Hungary

Correspondence: Endre V. Nagy, MD, PhD, DSc, Division of Endocrinology, Department of Internal Medicine, Faculty of Medicine, University of Debrecen, Nagyerdei krt. 98, 4032 Debrecen, Hungary. Email: nagy@internal.med.unideb.hu.

Abstract

Context: Increased orbital tissue volume due to matrix expansion, orbital fibroblast (OF) proliferation, and adipocyte differentiation are the hallmarks of thyroid eye disease (TED). Their combination with the presence of hyaluronan-bound excess water in the constrains of the bony orbit results in increased intraorbital pressure. High intraorbital pressure, along with changes in the mechanical properties of orbital tissues, may lead to the activation of mechanosensitive receptors. The expression and role of the Piezo1 mechanoreceptor has not been investigated in TED.

Objective: We aimed to verify the expression of Piezo1 in OFs, and to study the effect of in vitro Piezo1 activation by its synthetic agonist Yoda1 on adipocyte differentiation.

Methods: OF cultures established using orbital connective tissues from patients with TED and controls were studied in the presence or absence of adipogenic stimuli. Piezo1 expression was confirmed by Western Blot and immunofluorescent imaging, and its function was verified by intracellular Ca^{2+} measurement. Adipogenic differentiation was characterized using Oil Red O staining for lipid accumulation, real-time polymerase chain reaction for gene and Western blot for protein expressions indicative in adipogenesis.

Results: OFs express functional Piezo1 channels. Differentiation into adipocytes is inherent to TED OFs. Piezo1 activation by Yoda1 inhibits the expressions of early (CEBPβ, CEBPδ) and main (PPARγ, CEBPα) transcription factors, and the terminal marker FABP4 during adipogenesis, resulting in markedly lower intracytoplasmic lipid accumulation.

Conclusion: Piezo1 channels are expressed and functional in OFs. Modeling orbital pressure by in vitro Piezo1 activation reduces de novo adipogenesis of OFs derived from TED orbits.

Key Words: orbital fibroblasts, adipogenesis, Piezo1, Yoda1, PPARγ, Graves orbitopathy

Abbreviations: CEBP, CCAAT enhancer binding protein; DMEM, Dulbecco's modified Eagle's medium; ECM, extracellular matrix; FABP4, fatty acid binding protein 4; FBS, fetal bovine serum; MTT, 3-(4,5-dimethyl-2-thiazolyl)-2,5-diphenyl-2H-tetrazolium bromide; OF, orbital fibroblast; ORO, Oil Red O; PBS, phosphate-buffered saline; PPARγ, peroxisome proliferator activated receptor gamma; TAZ, transcriptional coactivator with PDZ-binding motif; TED, thyroid eye disease; TSHR, thyroid-stimulating hormone receptor; YAP, Yes-associated protein.

Thyroid eye disease (TED) is an autoimmune inflammatory disease of the orbital tissues driven by autoantibodies against the thyroid-stimulating hormone receptor (TSHR) expressed on orbital fibroblasts (OFs) (1). The activation of OFs, which leads to increased proliferation rate, excessive hyaluronan production, and increased adipocyte differentiation, is the key factor in the expansion of the orbital content in TED (2). The increased orbital adipose tissue volume is a result of increased number of newly formed adipocytes and enlargement of cell size due to lipid accumulation (3). Orbital tissues from patients with TED express higher amounts of adipocyte-related factors such as leptin, adiponectin, and peroxisome proliferator activated receptor gamma (PPARγ) than healthy orbital tissues. Moreover, these expression levels correlate positively with the TSHR expression (4), since adipogenesis increases TSHR expression (5). The transcriptional regulation of adipogenesis begins with the induction of CCAAT enhancer binding protein (CEBP) β and δ expression, which then activate PPARγ and CEBPα, the key factors in adipocyte differentiation with a synergistic effect on adipogenesis-related gene expression (6, 7). The lipid accumulation leads to the expression of fatty acid binding protein 4 (FABP4), which is a terminal marker of adipogenesis (8). Increased intraorbital pressure is a hallmark of TED, which may rise from 4 to 27 mmHg during the course of the disease (9); in severe cases, compression of the optic nerve and decreased or inverted venous blood flow in the major orbital vessels may result (10).

It has not been studied in detail yet if and how increased intraorbital pressure affects orbital tissue remodeling in TED. The single study that tried to reveal the connection of adipogenesis and pressure found that mechanical pressure had no

Received: 14 March 2024. **Editorial Decision:** 24 December 2024. **Corrected and Typeset:** 15 January 2025

significant effect on adipogenesis in 3D OF cultures (11). During the course of TED, different mechanical stimuli reach the OFs, which can lead to the activation of mechanosensitive receptors. Piezo1 is an inherently mechanosensitive Ca^{2+}-permeable nonselective cation channel (12). It has a 3-bladed propeller-like structure (13) and transforms mechanical stimuli into electrical and chemical signals (14). Its activity can be modulated by synthetic small molecules (eg, Yoda1 and Dooku1) (15, 16). Piezo1 activation with Yoda1 treatment decreases adipogenic differentiation of mesenchymal stem cells (17), brown adipocytes (18), human and mouse adipocytes (19), and perivascular adipose tissue preadipocytes (20).

We assume that in addition to the autoimmune process and changes in thyroid hormone levels, the increased intraorbital pressure and mechanical stimuli originating from the remodeled extracellular matrix (ECM) also play an important role in the pathogenesis of TED. These mechanical effects can be investigated, at least partly, by activating the Piezo1 channel, whose presence and function have not been confirmed in OFs yet. Our aim was to study the expression of Piezo1 in OFs and the effect of Piezo1 activation on adipogenic differentiation of OFs.

Materials and Methods

Materials

Dulbecco's Modified Eagle Medium (DMEM):F12, stable glutamine supplement, Dulbecco's phosphate-buffered saline without calcium and magnesium, and fetal bovine serum (FBS) were purchased from Biosera (Nuaille, France). TrypLE Express was purchased from Gibco (Thermo Fisher Scientific, Waltham, MA, USA). Biotin, pantothenic acid, dexamethasone, isobutyl methylxanthine, insulin, rosiglitazone, triiodothyronine, dimethyl sulfoxide, formaldehyde solution (37%), glycine, TritonX-100 and Oil Red O (ORO) stain, and Laemmli sample buffer were purchased from Sigma Aldrich (St. Louis, MO, USA). Yoda1 and Dooku1 were purchased from Tocris (Bio-Techne, Minneapolis, MN, USA). TRI reagent solution was purchased from Molecular Research Center Inc. (Cincinnati, OH, USA). High-Capacity cDNA Reverse Transcription Kit and TaqMan Gene Expression Assays were purchased from Applied Biosystems. Piezo1 antibody (Cat# MA5-32876, RRID:AB_2802511), GAPDH antibody (Cat# 39-8600, RRID:AB_2533438), Cyanine3 fluorophore-conjugated secondary antibody (Cat# A10521, RRID:AB_10373848), CEBPδ antibody (Cat# MA5-51237, RRID:AB_3093895), CEBPβ antibody (Cat# MA5-15893, RRID:AB_11152205), and Restore PLUS Western Blot Stripping Buffer were purchased from Thermo Fisher Scientific (Waltham, MA, USA). Goat antimouse IgG (H + L)–HRP (horseradish peroxidase) conjugate (Cat# 170-6516, RRID:AB_2921252) and goat antirabbit IgG (H + L)–HRP conjugate (Cat# 170-6515, RRID:AB_11125142) were purchased from BioRad (Hercules, CA, USA). PPARγ antibody (Cat# sc-7273, RRID:AB_628115) and CEBPα antibody (Cat# sc-166258, RRID:AB_2078042) were purchased from Santa Cruz Biotechnology (Santa Cruz, CA, USA).

Tissue Samples and Cell Cultures

Tissue samples from patients who underwent orbital surgery were obtained at the Department of Ophthalmology, University of Debrecen. All patients provided written informed consent, and the study was approved by the Ethics Committee of the Hungarian Medical Research Council with ID 5913/2012/EKU (84/13). The TED OF cultures (n = 5) originated from orbital connective tissue removed during decompression surgery from patients (3 females and 2 males) with inactive TED. The median age was 57 (min: 44, max: 63) years. The median TED duration from disease onset was 3 (min: 1, max: 8) years. All patients had inactive TED at the time of surgery (clinical activity score ≤ 3). For the control of their hyperthyroidism, all patients with TED received thyreostatic medication earlier or at the time of orbital surgery. One patient received radioiodine therapy and 2 patients underwent thyroidectomy. All received at least 1 full course of intravenous glucocorticoid treatment (21) and 1 of them underwent orbital irradiation; no glucocorticoid treatment or irradiation was performed during the last 12 months before orbital surgery. The source of normal OF cultures (NON-TED OFs; n = 5; 2 females and 3 males) was connective tissue obtained during enucleation surgery performed in patients with no thyroid or orbital diseases. The median age of NON-TED patients was 66 (min: 38, max: 82) years.

Primary human OF cultures were established as we described elsewhere (22) and kept frozen until used. OFs were cultured and differentiated into adipocytes using the following protocol. Cells were seeded in cell culture plates at 20 000 cells/cm^2 density, and incubated for 3 days in DMEM:F12 with 10% FBS (complete medium). Then, the culture medium was replaced with differentiation medium, which consisted of DMEM:F12 containing 10% FBS supplemented with 1.7 µM insulin, 33 µM biotin, 17 µM pantothenic acid, 1 nM triiodothyronine, and 10 µM rosiglitazone. For the first 4 days of the differentiation, 250 µM isobutyl methylxanthine and 10 µM dexamethasone were used as inducers of adipogenesis. Differentiation was continued for another 8 days; the medium with or without 10 µM Yoda1 or/and 10 µM Dooku1 was replaced every 4 days. Total RNA and protein of the cells was harvested just before addition of differentiation medium (day 0) and on the fourth, eighth, and twelfth days of adipogenesis. All experiments were performed at least 3 times and carried out in triplicate. Not all cell cultures were included in all measurements.

Oil Red O Staining

For measuring the rate of lipid accumulation, ORO staining was performed on day 0, 4, 8, and 12. Briefly, 10% formalin was added to cells after washing with phosphate-buffered saline (PBS). After fixation the cells were washed with ddH_2O, and the ORO solution was added for 20 minutes (23). After washing with ddH_2O and imaged with a Leica Leitz DMIL microscope (Leica Microsystems, Wetzlar, Germany), the ORO-stained lipids were dissolved in 2-propanol and the absorbance measured at 490 nm using Synergy H1 Microplate Reader (Agilent Technologies Inc. Santa Clara, CA, USA). Lipid accumulation was expressed as the optical density of dissolved dye per well.

Metabolic Activity Assay

The cells were treated with differentiation medium with or without Yoda1 for 12 days. The 3-(4,5-dimethyl-2-thiazolyl)-2,5-diphenyl-2H-tetrazolium bromide (MTT) assay was

performed on day 0, 4, 8, and 12 of the adipogenesis protocol. Briefly, MTT was added at a final concentration of 0.5 mg/mL, and the cells were incubated for 3 hours in a CO_2 incubator at 37 °C. The blue formazan crystals formed as a result of the metabolic activity of the cultured cells were dissolved in dimethyl sulfoxide. The absorbance at 550 nm (reference wavelength: 660 nm) was detected using Synergy H1 Microplate Reader.

Real-Time Polymerase Chain Reactions

The RNA was isolated using TRI reagent combined with chloroform extraction. For making the cDNA library a high-capacity cDNA reverse transcription kit was used. The TaqMan Gene Expression Assay was used for the detection of the expression of adipogenesis-related genes: CEBPβ (Hs00942496_s1), CEBPδ (Hs00270931_s1), CEBPα (Hs00269972_s1), PPARγ (Hs01115513_m1), and FABP4 (Hs01086177_m1). The results were normalized to GAPDH (Hs02758991_g1) mRNA levels by the ΔCT method. The reactions were performed by the CFX Opus 96 real-time polymerase chain reaction system (BioRad, Hercules, CA, USA).

Immunolabeling, Confocal Imaging

OFs were fixed with 4% paraformaldehyde for 15 minutes. After fixation, 100 mM glycine in PBS was used to neutralize excess amounts of paraformaldehyde. Fixed OFs were permeabilized with 0.5% TritonX-100 for 10 minutes and 10-minute-long washing was used 3 times with PBS. Nonspecific binding sites were blocked with Carbo-Free solution (SP-5040, VECTOR Laboratories, Burlingame, CA, USA) for 60 minutes at room temperature. Primary antibody, anti-PIEZO1 (Thermo Fisher Scientific, Rockford, IL, USA, MA5-32876, mouse-IgG, monoclonal), was incubated with the OFs overnight on 4 °C. Samples were washed 3 times with PBS and incubated with Cyanine3 fluorophore-conjugated secondary antibodies (A10521, Life technologies, Eugene, OR, USA) at room temperature for 1 hour. After washing 3 times, mounting was performed with 45 µL of mounting medium (H-1200, Vecta Shield + DAPI, Vector Laboratories). Image acquisition was done with an AiryScan 880 laser scanning confocal microscope (Zeiss, Oberkocken, Germany) equipped with a ×63 immersion oil objective. Excitation at 405 (DAPI) and 543 (Cy3) nm wavelengths was used to detect fluorescence. Paraffin sections of connective tissue samples were deparaffinized before treatment with a series of graded alcohol solutions. Although these sections were already fixed, they were postfixed as described above. After the final washing step and before covering the slides, autofluorescence quenching was performed on the samples with a Vector TrueVIEW autofluorescence quenching kit (SP-8400-15).

Western Blotting

The protein was isolated using TRI reagent according to manufacturers' instructions. Twofold concentrated Laemmli sample buffer (Sigma Aldrich) was added to isolated samples and boiled for 5 minutes at 95 °C. A 20-µg bolus of total protein was loaded into the wells of the 7.5% sodium dodecyl sulfate–polyacrylamide gel for Piezo1 or 10% TurboMix Bis-Tris casting gel (Merck KGaA, Darmstadt, Germany) for other target proteins. Proteins were transferred into a nitrocellulose membrane with Trans-Blot Turbo Transfer System (BioRad, Hercules, CA, USA). Nonspecific binding sites were blocked with 0.5% nonfat milk powder dissolved in PBST (PBS supplemented with 0.1% Tween-20). Primary antibodies (Piezo1, CEBPβ, CEBPδ and CEBPα, PPARγ, GAPDH) were probed for 10 minutes using the SNAP id 2.0 system (Merck KGaA, Darmstadt, Germany). After washing with the SNAP id 2.0 system 4 times for 20 seconds in PBST, membranes were incubated with HRP-conjugated secondary antibodies for 10 minutes. Each membrane was stripped and reprobed up to 3 times using Restore PLUS Western Blot Stripping Buffer; the last probe was always GAPDH. Luminescence signals were detected using enhanced chemiluminescence kit WesternSure Premium Chemiluminescent Substrate (LI-COR Biotechnology GmbH, Bad Homburg, Germany) in a C-DiGit Blot Scanner (LI-COR Biotechnology GmbH). The results of the densitometric analyses were presented as the relative ratio of measured proteins to GAPDH, which was labeled in every membrane.

Measurement of Intracellular Ca^{2+} Concentration in Cultured Fibroblast Cells

Cells from primary fibroblast cultures were loaded with 10 µM Fura-2-AM for 20 minutes at 37 °C. After loading the cells were kept in Tyrode's solution. Fura-2 was excited with a CoolLED pE-340fura light source (CoolLED LTD, Andover, UK) mounted on a ZEISS Axiovert 200 inverted microscope (Zeiss, Oberkochen, Germany). The excitation wavelengths were alternating between 340 and 380 nm wavelength, and the emission was detected with a bandpass filter between 505 and 570 nm. Image acquisition and postprocessing were made with AxioVision (rel. 4.8) software (Zeiss, Oberkochen, Germany). The $Ca2^{+}$ concentration was estimated from the ratio of the images taken at 340 and 380 nm with background correction.

Statistical Analysis

STATISTICA software (TIBCO Software Inc., Palo Alto, CA, USA) was used to perform the statistical analyses. Student's t-test or repeated measures ANOVA followed by the Fisher LSD post hoc test was used to evaluate the differences between groups. Data are presented as mean ± standard error of mean (SEM). Statistical significance was accepted at the 5% level ($P < .05$).

Results

Expression of Piezo1 Channels in Orbital Connective Tissue and Orbital Fibroblasts

We confirmed that orbital connective tissues and OFs from TED and NON-TED patients express Piezo1 protein (Fig. 1A and 1B, respectively). Piezo1 mRNA expression was present in OFs and their GAPDH-normalized expression levels did not differ according to their TED (n = 3) or NON-TED (n = 4) origin ($P = .29$). The presence of Piezo1 protein in OFs was confirmed by Western blot; densitometric analysis revealed that there is no difference in the Piezo1 protein expression between the TED and NON-TED OFs ($P = .338$) (Fig. 1C and 1D). The effect of Piezo1 agonist, Yoda1 on Ca^{2+} influx in OFs was tested to confirm that functional Piezo1 was expressed. Yoda1 increased the intracellular Ca^{2+} level to a similar extent in TED OFs and NON-TED OFs (Fig. 2A and 2B).

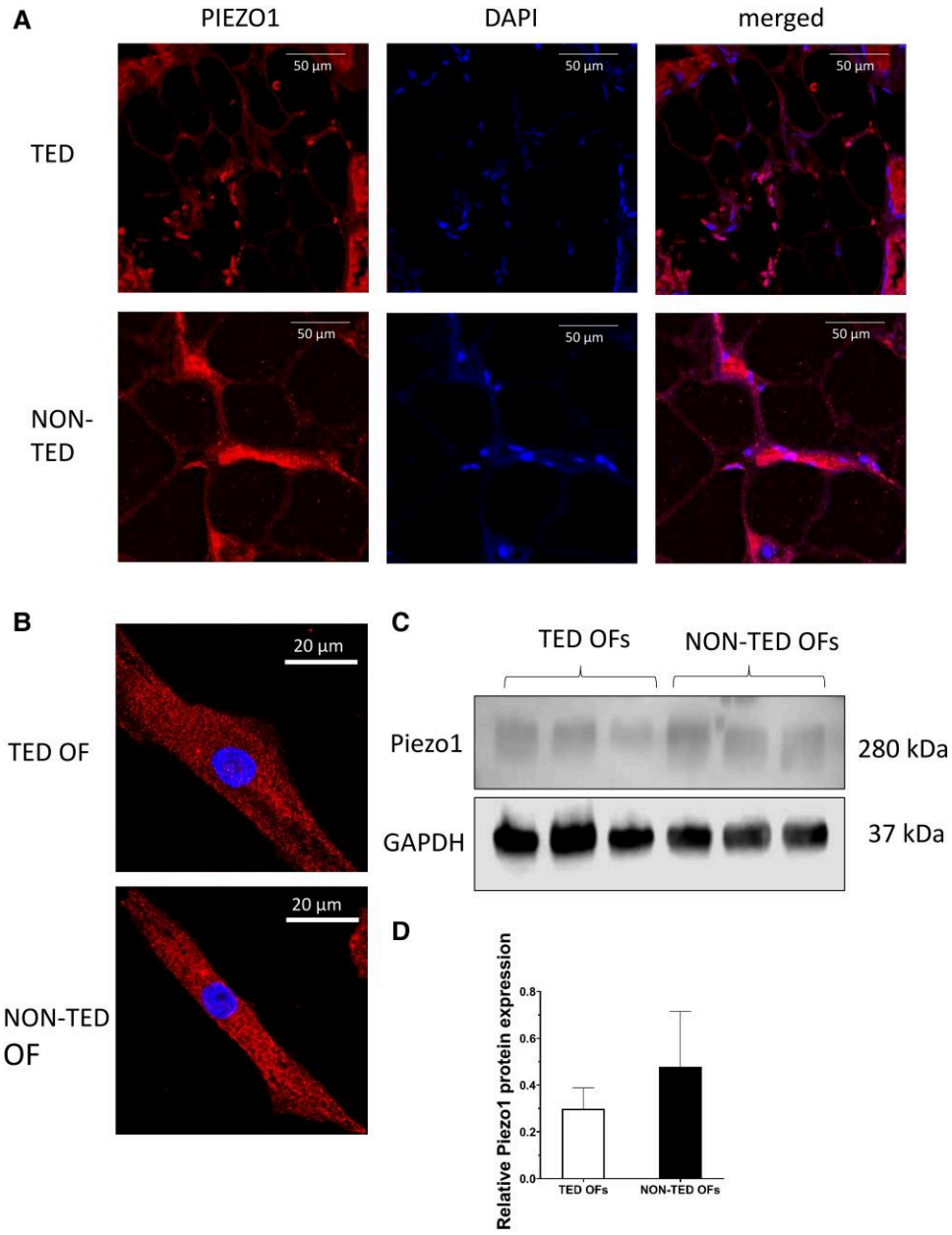

Figure 1. Verification of the expression of Piezo1 in orbital connective tissue (A) and orbital fibroblasts (B). Fluorescent staining: Piezo1–Cy3, cell nuclei–DAPI. (C) Western blot analysis (C) and densitometric data (D) of Piezo1 protein expression in TED OFs (n = 3) and NON-TED OFs (n = 3). Samples were immunoblotted for Piezo1 and reprobed with antibody for GAPDH for normalization of loaded protein levels. The values are expressed as mean ± SEM.

Abbreviations: TED OFs, thyroid eye disease orbital fibroblasts; NON-TED OFs, normal orbital fibroblasts; GAPDH, glyceraldehyde 3-phosphate dehydrogenase.

The Effect of Piezo1 Activation on the Adipogenesis of Orbital Fibroblasts

During adipogenesis lipid accumulation was increased as evidenced by the elevation in ORO staining compared with day 0 in every time point studied (Fig. 3A). Under basal conditions (day 0) and after 4 days of induction, ORO staining in TED and NON-TED OFs did not differ, but the rate of its subsequent increase in OFs of different origin diverged (Fig. 3A). Lipid accumulation in NON-TED OF cultures during the differentiation protocol was substantially lower than in TED OF cultures (Fig. 3C and 3D). Yoda1 treatment decreased ORO staining at days 8 and 12 of adipogenesis in TED OFs (Fig. 3A and 3E), but had no effect in NON-TED OFs where lipid accumulation was at an intrinsically low level (Fig. 3A and 3F). The basal expression of the terminal marker of adipogenesis, FABP4 (Fig. 3B), did not differ in the different cell types. Its rise was negligible in NON-TED OFs compared with TED OFs on days 8 and 12, the latter exhibiting a marked increase. Yoda1 had no effect on FABP4 expression on day 4 but decreased it in both TED and NON-TED OFs on day 8, but only in TED OFs on day 12.

To analyze mRNA expression underlying the observed changes, at first, we examined the important early regulatory factors of adipogenesis, CEBPβ and CEBPδ (Fig. 4A and 4B). Basal CEBPβ expressions did not differ in OFs with different origins, while basal CEBPδ expression was lower in TED

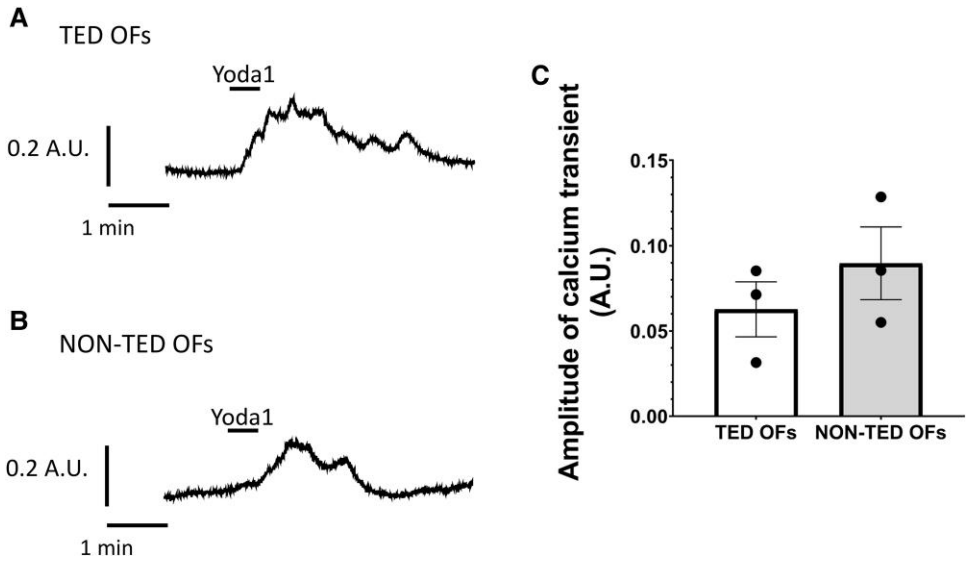

Figure 2. Verification of the functionality of the Piezo1 channel in samples from healthy and diseased individuals. Representative calcium transients recorded on Fura2-loaded cells following Yoda1 application in OFs originated from (A) TED and (B) NON-TED patients. (C) The amplitudes of calcium transients showed no significant difference between OFs with different origin (TED OFs, n = 3 and NON-TED OFs, n = 3). The values are expressed as mean ± SEM.

Abbreviations: TED OFs, thyroid eye disease orbital fibroblasts; NON-TED OFs, normal orbital fibroblasts.

OFs than in NON-TED OFs. After 4 days of induction, the CEBPβ expression of NON-TED OFs decreased, and remained reduced during the studied 12-day period, while CEBPβ mRNA levels increased in TED OFs during the first 4 days and did not change afterwards. CEBPδ expression showed an increase only in TED OFs on days 4 and 8, compared with the levels measured on day 0; the expression levels descended to the initial levels by day 12. In TED OFs, Yoda1 treatment inhibited mRNA expression of both factors on days 4 and 8 while on the day 12 it only acted on CEBPβ expression. In contrast, in NON-TED OFs, Yoda1 did not affect the expression levels of CEBPβ and CEBPδ.

Next, we examined PPARγ and CEBPα (Fig. 4C and 4D) mRNA expressions, which are the main regulators in the second wave of the adipogenic cascade. In our experiments the origin of the fibroblasts (TED or NON-TED) had no influence on basal PPARγ and CEBPα expression. Under the effect of adipogenic conditions, PPARγ and CEBPα expression increased in OFs. In TED OFs, compared with NON-TED OFs, the increase in PPARγ was higher in every time point examined. PPARγ mRNA expression did not change after 4 days of Yoda1 treatment in OFs, while we found a reduced CEBPα expression on day 4 in TED and NON-TED OFs compared with cultures in adipogenic media without Yoda1. On day 8 Yoda1 inhibited PPARγ expression in both cell types, while CEBPα was reduced only in TED OFs; on day 12, the expression levels of both regulators decreased only in TED OFs.

We performed Western blot analysis in order to measure the protein levels of transcription factors on day 12; the inhibitory effect of Yoda1 treatment on mRNA expressions of adipogenic transcription factors were reflected in protein levels. Further, both mRNA expressions (Fig. 4) and protein levels of the transcription factors CEBPβ, CEBPδ, CEBPα, and PPARγ reduced only in TED OFs (Fig. 5C and 5D) by the end of day 12 of adipogenic differentiation. In addition, we found lower CEBPβ, α, and PPARγ protein levels in nondifferentiating NON-TED OFs than in TED OFs.

In order to clarify whether timing of Piezo1 activation modifies its inhibitory effect on the adipogenesis of TED OFs (n = 3), we repeated the experiment limiting Yoda1 exposure to the first 4 days (adipogenesis induction), and, in another set, for the subsequent 8 days only. We found that when Yoda1 treatment was withdrawn after the induction phase, it did not affect the lipid accumulation of the cells (ORO: $P = .776$, PPARγ: $P = .090$, FABP4: $P = .328$). However, if Piezo1 was activated after induction and was present during the last 8 days, it reduced lipid accumulation, and PPARγ and FABP4 expression ($P < .01$, $P < .01$, $P < .01$, respectively) compared with vehicle-treated differentiated cells. The adipogenesis-inhibiting effect was similar if Yoda1 exposure was limited for the last 8 days or the whole duration of adipogenesis (data not shown).

Piezo1 Activation has no Effect on Cell Viability

In order to show that the decrease in ORO staining and mRNA expression levels were not due to the cytotoxic effect of 10 μM Yoda1 treatment, the MTT assay was performed. The metabolic activity increased with time under adipogenic conditions in the absence of Yoda1: 1.58 ± 0.04-fold on day 4, 2.67 ± 0.45-fold on day 8, and 3.34 ± 0.37-fold on day 12 compared with day 0 (expressed as mean ± SD). Yoda1 treatment further increased (mean 1.21 ± 0.03-fold) the metabolic activity in both cell types by day 4. On days 8 and 12 there was no statistical difference in the metabolic activity between untreated and Yoda1 treated cells (data not shown).

Dooku1 Diminishes the Inhibitory Effect of Yoda1

To confirm that the decrease of adipogenesis was related to Piezo1 activation, we used Dooku1, a competitive inhibitor of Yoda1. Only cultures that have exhibited marked adipogenesis (ie, TED OFs) were included in this experiment. The coapplication of Dooku1 (10 μM) with Yoda1 substantially hampered Yoda1's reducing effect on both lipid accumulation (Fig. 6A) and FABP4 expression (Fig. 6B). Dooku1 treatment

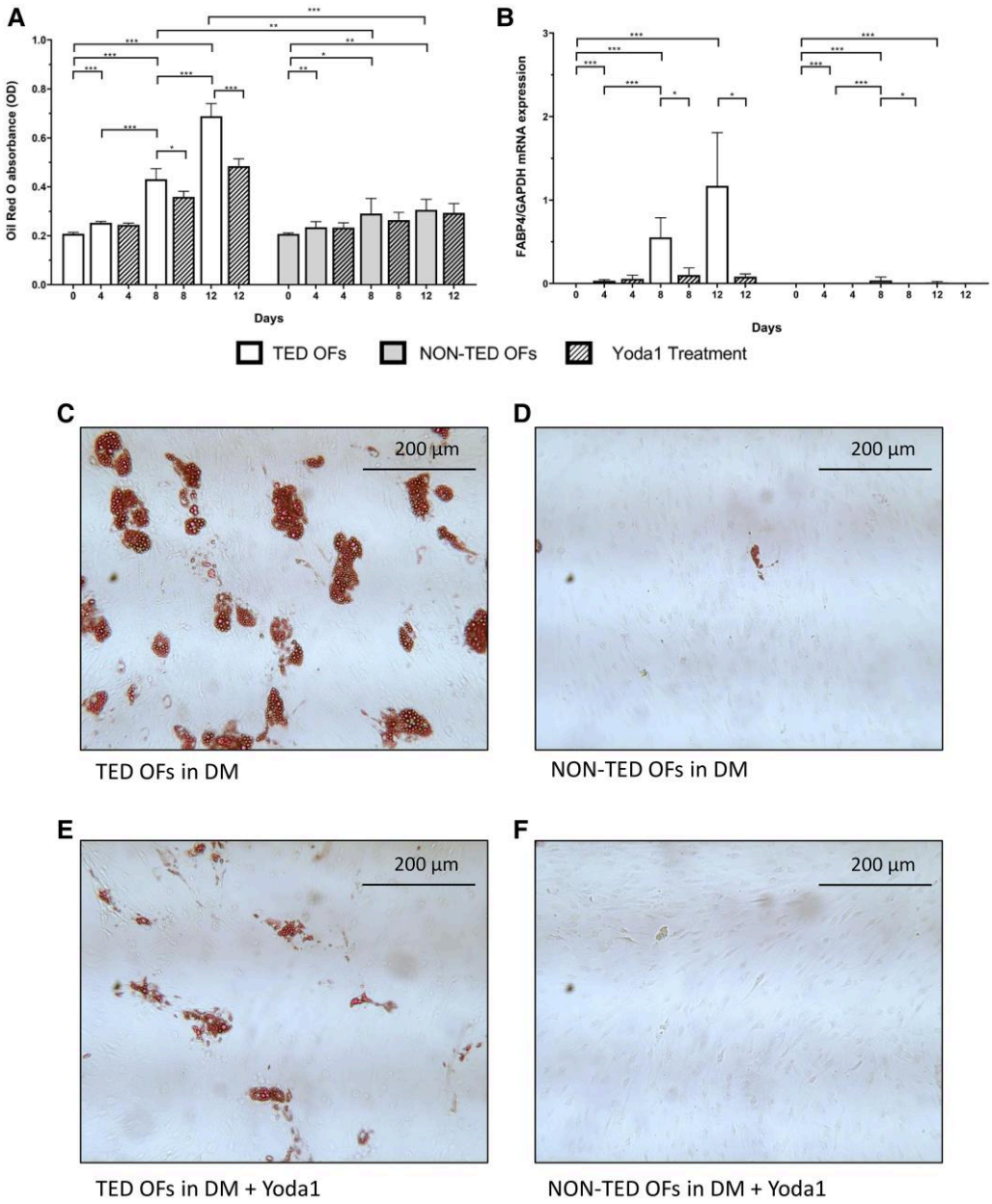

Figure 3. Lipid accumulation during adipogenesis in orbital fibroblasts. (A) ORO staining in TED (n = 5) and NON-TED OFs (n = 5) before initiation (day 0) and on the fourth, eighth, and twelfth day of adipogenesis by spectrophotometric measurement of the dissolved ORO dye. (B) The mRNA expression of terminal marker FABP4 in TED OF (n = 3) and NON-TED OFs (n = 4). (C-F) Representative ORO staining of TED and NON-TED OFs on day 12 of adipogenesis cultured in the absence (B and C) and presence of (D and E) of Yoda1. The values are expressed as mean ± SEM. $*P < .05$; $**P < .01$; $***P < .001$.

Abbreviations: TED OFs, thyroid eye disease orbital fibroblasts; NON-TED OFs, normal orbital fibroblasts; ORO, Oil Red O staining; DM, differentiation medium; FABP4, fatty acid binding protein 4.

alone did not alter lipid accumulation measured with ORO staining and FABP4 expression in TED OFs.

The Effect of Adipogenic Stimuli on Piezo1 Expression

Piezo1 protein expression is increased with time, both in complete and in differentiation medium (Fig. 7). Under the adipogenic stimuli compared with cells maintained in complete medium, the behavior of TED and NON-TED OFs differs on day 4, as we found a decrease in Piezo1 expression in TED OFs, but not in NON-TED OFs. On day 8, based on the densitometric data, we found a tendency to increasing Piezo1 expression in OFs in differentiation medium compared with complete medium, but it failed to reach statistical significance.

Discussion

TED is characterized by soft tissue volume enlargement in the bony orbit due to the large amount of hyaluronan produced by activated OFs, increased OF proliferation, and differentiation of OFs into adipocytes (24). Orbital anatomy limits tissue expansion at the cost of increased pressure, resulting in a constant mechanical stimulus for orbital soft tissues. Theoretically, if pressure increases in the orbit, protective

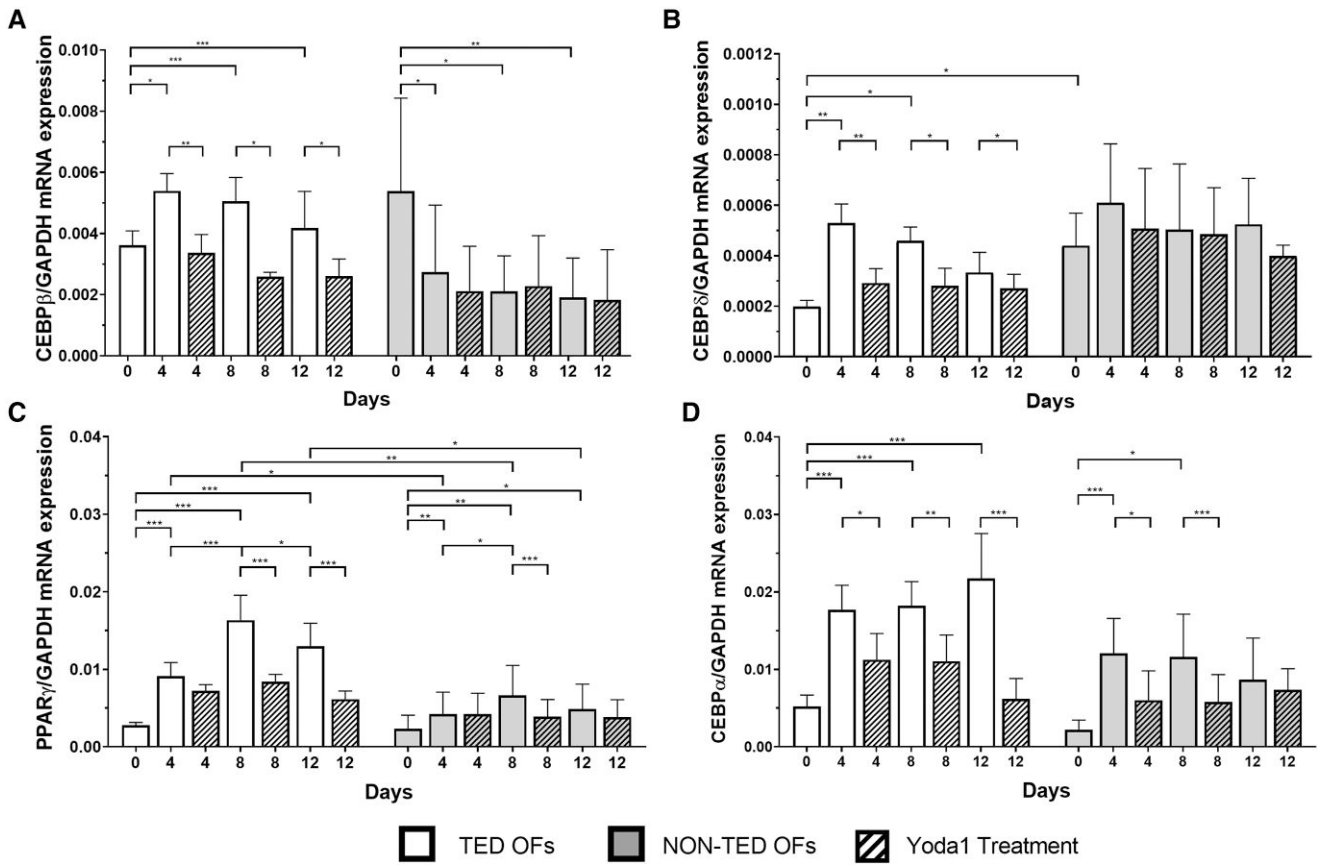

Figure 4. The effect of Yoda1 treatment on the mRNA expressions of adipogenesis related transcription factors in TED OFs (n = 3) and NON-TED OFs (n = 4) (A-D). The values are expressed as mean ± SEM. $*P < .05$; $**P < .01$; $***P < .001$.

Abbreviations: TED OFs, thyroid eye disease orbital fibroblasts; NON-TED OFs, normal orbital fibroblasts; ORO, Oil Red O staining; C/EBP, CCAAT enhancer binding proteins; PPARγ, peroxisome proliferator-activated receptor gamma; GAPDH, glyceraldehyde-3-phosphate dehydrogenase.

mechanisms should prevent the processes of additional tissue expansion. In the present study, we have focused on adipogenic differentiation, as after differentiation an adipocyte occupies substantially larger volume than its predecessor fibroblast; inhibiting adipocyte differentiation may be a means of hindering further rise in orbital pressure.

Mechanosensitive receptors, including Piezo1, have important roles in mechanotransduction that influence cell proliferation and differentiation (25). We used OFs to set up an in vitro model to characterize the effect of mechanical stimuli via Piezo1 activation on adipogenic differentiation of OFs. Activation by synthetic molecules is proven to be a useful tool to study the effects of mechanical stimuli via Piezo1 in different cell types (18, 20, 26). Using immunohistochemistry, we confirmed that TED and NON-TED orbital connective tissues express Piezo1 protein. We found that OFs in cultures established from orbital connective tissue express functional Piezo1 channels (Figs. 1 and 2); furthermore, the activation of Piezo1 decreased lipid accumulation during adipogenesis (Fig. 3).

Piezo1 is present on most cell types, including cardiomyocytes, immune cells, and endothelial and vascular smooth muscle cells, and has a major role in normal cell physiology. In addition to direct physical force, Piezo1 is responsible for sensing the changes in ECM stiffness and intracellular mechanical stimuli originated from cytoskeletal remodeling (27). It has been revealed that mechanical stimuli had an effect on adipogenesis-related genes: in 3T3-L1 cells stretching decreased PPARγ expression, while mRNA levels of CEBPα and CEBPβ did not change (28). In preadipocytes, expression of PPARγ and CEBPα is inhibited after application of a compressive force whereas CEBPβ and δ remained unchanged (29). We found that Piezo1 stimulation by Yoda1 markedly inhibited adipocyte differentiation in TED OFs: Yoda1 treatment had an inhibitory effect on the expressions of early adipogenesis genes, CEBPβ and CEBP δ, and also on master regulators, PPARγ and CEBPα, at both mRNA and protein levels, and then consequently on the terminal marker FABP4.

Our observation that the inhibitory effect of Yoda1 treatment was weakened by using it only during the induction of adipogenesis (day 0-4) compared with longer treatments (day 0-12 and day 4-12) indicates that Piezo1 activation is not inevitable at the induction of adipogenesis to exert its inhibitory effect.

The use of the Piezo1 activation antagonist, Dooku1, hindered Yoda1-induced suppression of adipocyte differentiation. Our results are consistent with previous studies in adipocytes with different anatomical origin (18, 20); we also confirm that Piezo1 activation decreases PPARγ expression and inhibits adipogenesis.

The main limitation of our study is that in our in vitro activation model we cannot estimate the combined effect of various mechanosensitive pathways activated by elevated orbital pressure; our approach is restricted to 1 component in the mechanotransduction process. The methods applied here are not suitable for examining the function disparity of Piezo1 between TED and NON-TED OFs.

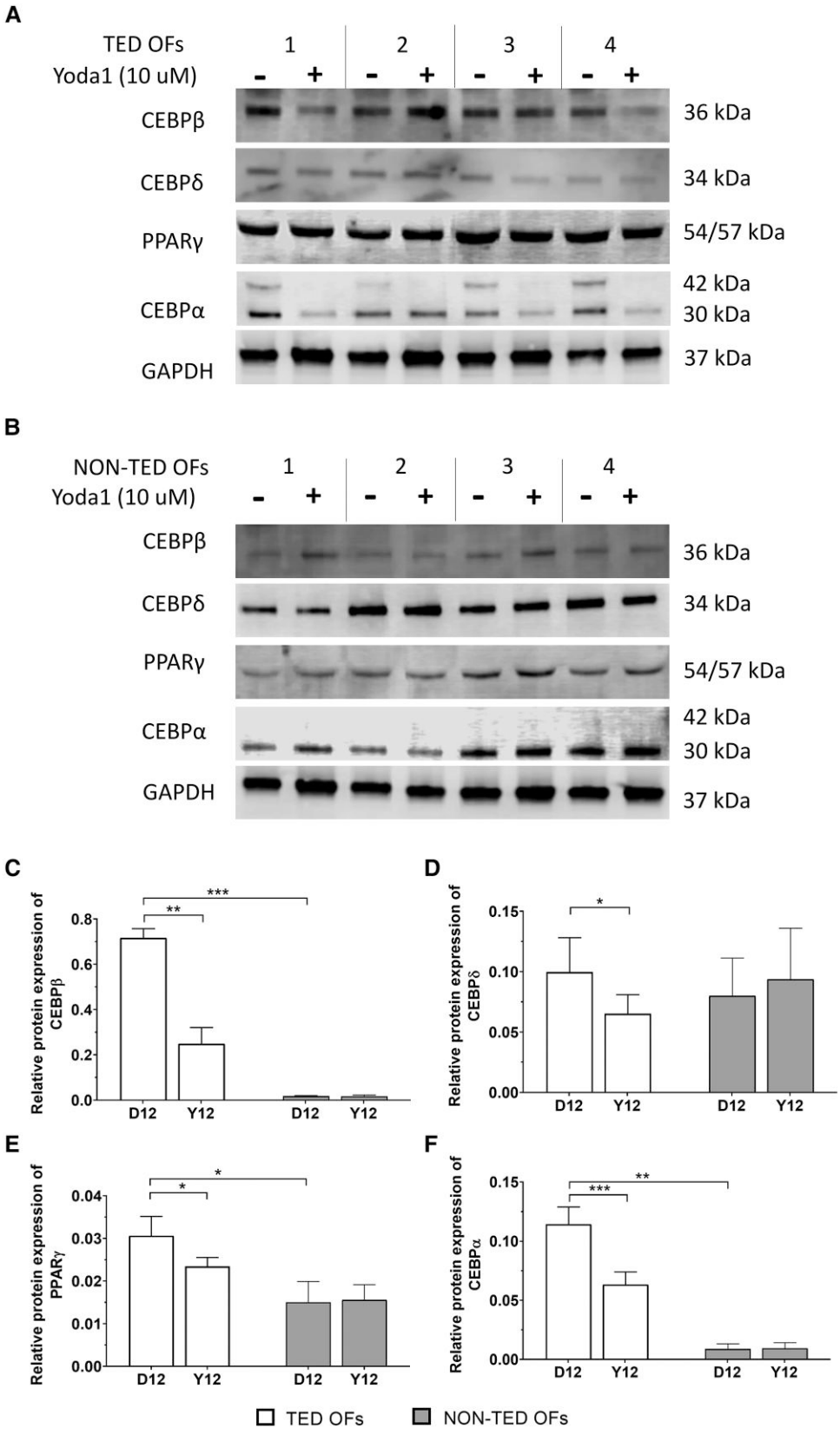

Figure 5. Western blot analysis of protein expression levels of adipogenic transcription factors, CEBPβ, CEBPδ, PPARγ, and CEBPα in TED OFs (n = 4) (A) and NON-TED OFs (n = 4) (B) treated for 12 days using adipogenic stimuli. Representative gel images are shown. Densitometric data of adipogenesis-related proteins (C-F); GAPDH was used on each membrane for normalization. The values are expressed as mean ± SEM. $^{*}P < .05$; $^{**}P < .01$; $^{***}P < .001$.

Abbreviations: TED OFs, thyroid eye disease orbital fibroblasts; NON-TED OFs, normal orbital fibroblasts; CEBP, CCAAT enhancer binding proteins; PPARγ, peroxisome proliferator-activated receptor γ; GAPDH, glyceraldehyde-3-phosphate dehydrogenase.

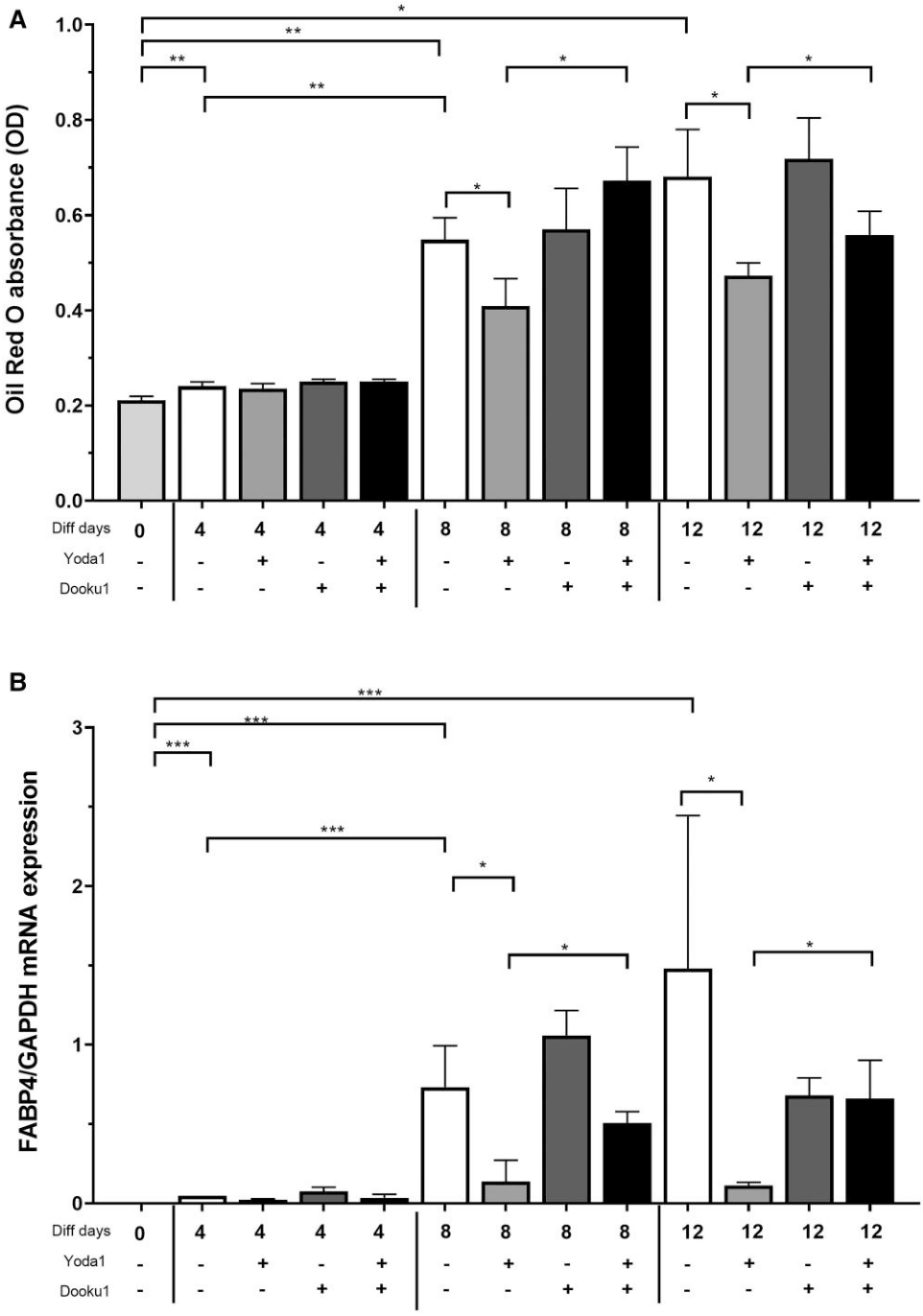

Figure 6. The effect of Dooku1 treatment on Yoda1-inhibited lipid accumulation (A) and FABP4 terminal marker expression (B) in TED OFs (n = 2). The values are expressed as mean ± SEM. *$P < .05$; **$P < .01$; ***$P < .001$.

Abbreviations: TED OFs, thyroid eye disease orbital fibroblasts; OD, optical density; FABP4, fatty acid binding protein 4; GAPDH, glyceraldehyde-3-phosphate dehydrogenase.

In agreement with the findings of others (11, 30), markedly lower adipocyte differentiation was found in NON-TED OFs than in TED OFs; our observation regarding the inhibitory effect of Piezo1 activation on adipogenesis is based on the results obtained in TED OFs. None of the studied parameters measured on day 0 explained the differences between TED and NON-TED OFs. However, it was outside the scope of this study to identify the factors responsible for the different behavior of TED and NON-TED OFs. We found that after adipogenic induction, the early adipogenic transcription factors CEBPβ and CEBPδ did not increase and the upregulation of factors in the next level (PPARγ and CEBPα) was moderate in NON-TED OFs compared with TED OFs. After the 12-day adipogenic protocol the protein levels of CEBPβ, CEBPα, and PPARγ were lower in NON-TED OFs than in TED OFs. These differences manifested as lower lipid accumulation verified by ORO staining and negligible expression of the terminal marker FABP4 in NON-TED OFs. Li et al confirmed that adipogenesis could be induced in NON-TED OFs using mechanical pressure stimuli in a pseudophysiological 3D environment (11), while modeling mechanical stimuli in our 2D cultures using in vitro Piezo1 activation with Yoda1 in NON-TED OFs

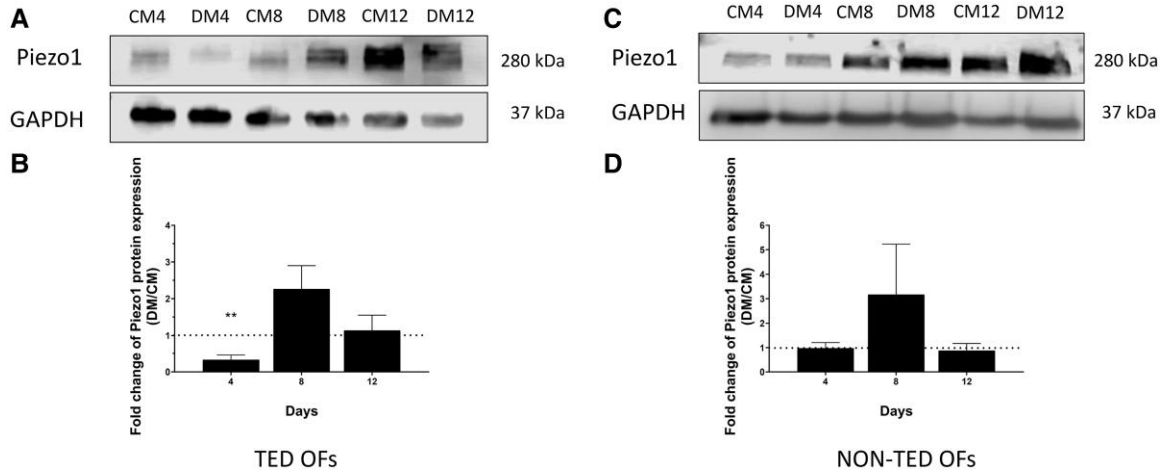

Figure 7. Changes of Piezo1 protein expression during adipogenesis. Representative Western blots (A and C) and the mean changes of Piezo1 protein expression of cell cultures under adipogenic stimuli compared with unstimulated cells, based on densitometric data (B and D). TED OFs (n = 3) and NON-TED OFs (n = 3) were maintained in complete medium or differentiation medium for 4, 8, and 12 days. Protein samples were immunoblotted for Piezo1 and reprobed with antibody for GAPDH for normalization of loaded protein levels. The values are expressed as mean ± SEM. $^{**}P < .01$.

Abbreviations: CM, complete medium; DM, differentiation medium; TED OFs, thyroid eye disease orbital fibroblasts; NON-TED OFs, normal orbital fibroblasts; GAPDH, glyceraldehyde 3-phosphate dehydrogenase.

had no essential effect on their susceptibility to adipogenic differentiation. We assume that Piezo1 activation alone in 2D cultures is not equivalent to a pressure stimulus on cells in a 3D matrix (ie, mechanical stimuli may have a greater effect than Yoda1 alone).

Organotypic microenvironment in 3D culture is beneficial for adipogenesis due to repression of some pathways with an inhibitory effect on adipogenic differentiation including Hippo and TGF-β signaling (31). Yes-associated protein (YAP) and transcriptional coactivator with PDZ-binding motif (TAZ) are parts of the Hippo pathway, and Piezo1 converts mechanical stimuli into biological signals through YAP and TAZ signaling, which are known mediators of mechanical cues (32-34). It is confirmed that suppression of adipogenesis occurred by increasing nuclear localization of YAP (35) and upregulation of TAZ (36), and in OFs it acts toward fibrosis (37). When the Piezo1 channel is open/active, the Ca^{2+} influx from the extracellular space initiates intracellular signal transduction (eg, via the YAP/TAZ pathway) (38). In addition, Ca^{2+} influx has an inhibitory effect on adipogenesis of 3T3-L1 cells (39) through the calcineurin pathway (40). It has already been described that the TGF-β (41) and WNT (42) signaling pathways also inhibit adipocyte differentiation. In other cell types it was confirmed that Piezo1 activation can upregulate TGF-β (43) and WNT signaling (44). Based on these data, we assume that in TED OFs Piezo1 activation may inhibit adipogenesis through the upregulation of YAP/TAZ, TGF-β, WNT, and calcineurin signaling but the exact mechanism needs to be clarified in future studies.

As far as we know, we are the first to show that the Piezo1 channel is expressed in orbital connective tissue. We confirmed that Piezo1 was functional in established OF cultures. We revealed that Piezo1 activation using Yoda1, as an in vitro model for increased orbital pressure, decreases adipogenic differentiation of OFs. mRNA and protein expression of 4 adipogenesis-related genes, including the early factors CEBPβ and CEBPδ, were inhibited by Yoda1. We conclude that mechanical stimuli including orbital pressure may reduce de novo adipogenesis during the course of TED via Piezo1 activation. This may be 1 way of how increasing pressure may keep expansion of the orbital content under control. Further studies on the role of mechanical forces in tissue remodeling in TED may verify details of their contribution to the pathogenesis of TED.

Funding

This research was funded by the Hungarian National Research, Development and Innovation Office, grant number: K143464. Project K143464 has been implemented with the support provided by the Ministry of Innovation and Technology of Hungary from the National Research, Development and Innovation Fund, financed under the K_22 funding scheme.

Disclosures

The authors have nothing to disclose.

Data Availability

Some or all datasets generated during and/or analyzed during the current study are not publicly available but are available from the corresponding author on reasonable request.

References

1. Bahn RS. Graves' ophthalmopathy. *N Engl J Med*. 2010;362(8):726-738.
2. Dik WA, Virakul S, van Steensel L. Current perspectives on the role of orbital fibroblasts in the pathogenesis of Graves' ophthalmopathy. *Exp Eye Res*. 2016;142:83-91.
3. Zhang C, Zhang X, Ma L, Peng F, Huang J, Han H. Thalidomide inhibits adipogenesis of orbital fibroblasts in Graves' ophthalmopathy. *Endocrine*. 2012;41(2):248-255.
4. Kumar S, Coenen MJ, Scherer PE, Bahn RS. Evidence for enhanced adipogenesis in the orbits of patients with Graves' ophthalmopathy. *J Clin Endocrinol Metab*. 2004;89(2):930-935.
5. Zhang L, Baker G, Janus D, Paddon CA, Fuhrer D, Ludgate M. Biological effects of thyrotropin receptor activation on human

orbital preadipocytes. *Invest Ophthalmol Vis Sci*. 2006;47(12):5197-5203.
6. Hamm JK, Park BH, Farmer SR. A role for C/EBPbeta in regulating peroxisome proliferator-activated receptor gamma activity during adipogenesis in 3T3-L1 preadipocytes. *J Biol Chem*. 2001;276(21):18464-18471.
7. Lefterova MI, Zhang Y, Steger DJ, *et al*. PPARgamma and C/EBP factors orchestrate adipocyte biology via adjacent binding on a genome-wide scale. *Genes Dev*. 2008;22(21):2941-2952.
8. Rosen ED, Walkey CJ, Puigserver P, Spiegelman BM. Transcriptional regulation of adipogenesis. *Genes Dev*. 2000;14(11):1293-1307.
9. Berthout A, Vignal C, Jacomet PV, Galatoire O, Morax S. [Intraorbital pressure measured before, during, and after surgical decompression in Graves' orbitopathy]. *J Fr Ophtalmol*. 2010;33(9):623-629.
10. Meyer P, Das T, Ghadiri N, Murthy R, Theodoropoulou S. Clinical pathophysiology of thyroid eye disease: the cone model. *Eye (Lond)*. 2019;2(2):244-253.
11. Li H, Fitchett C, Kozdon K, *et al*. Independent adipogenic and contractile properties of fibroblasts in Graves' orbitopathy: an in vitro model for the evaluation of treatments. *PLoS One*. 2014;9(4):e95586.
12. Coste B, Mathur J, Schmidt M, *et al*. Piezo1 and Piezo2 are essential components of distinct mechanically activated cation channels. *Science*. 2010;330(6000):55-60.
13. Zhao Q, Zhou H, Li X, Xiao B. The mechanosensitive Piezo1 channel: a three-bladed propeller-like structure and a lever-like mechanogating mechanism. *FEBS J*. 2019;286(13):2461-2470.
14. Cox CD, Bavi N, Martinac B. Origin of the force: the force-from-lipids principle applied to piezo channels. *Curr Top Membr*. 2017;79:59-96.
15. Evans EL, Cuthbertson K, Endesh N, *et al*. Yoda1 analogue (Dooku1) which antagonizes Yoda1-evoked activation of Piezo1 and aortic relaxation. *Br J Pharmacol*. 2018;175(10):1744-1759.
16. Syeda R, Xu J, Dubin AE, *et al*. Chemical activation of the mechanotransduction channel Piezo1. *Elife*. 2015;4:e07369.
17. Sugimoto A, Miyazaki A, Kawarabayashi K, *et al*. Piezo type mechanosensitive ion channel component 1 functions as a regulator of the cell fate determination of mesenchymal stem cells. *Sci Rep*. 2017;7(1):17696.
18. Kenmochi M, Kawarasaki S, Takizawa S, Okamura K, Goto T, Uchida K. Involvement of mechano-sensitive Piezo1 channel in the differentiation of brown adipocytes. *J Physiol Sci*. 2022;72(1):13.
19. Wang S, Cao S, Arhatte M, *et al*. Adipocyte Piezo1 mediates obesogenic adipogenesis through the FGF1/FGFR1 signaling pathway in mice. *Nat Commun*. 2020;11(1):2303.
20. Rendon CJ, Flood E, Thompson JM, Chirivi M, Watts SW, Contreras GA. PIEZO1 mechanoreceptor activation reduces adipogenesis in perivascular adipose tissue preadipocytes. *Front Endocrinol (Lausanne)*. 2022;13:995499.
21. Zang S, Ponto KA, Kahaly GJ. Clinical review: intravenous glucocorticoids for Graves' orbitopathy: efficacy and morbidity. *J Clin Endocrinol Metab*. 2011;96(2):320-332.
22. Galgoczi E, Jeney F, Gazdag A, *et al*. Cell density-dependent stimulation of PAI-1 and hyaluronan synthesis by TGF-β in orbital fibroblasts. *J Endocrinol*. 2016;229(2):187-196.
23. Yoon Y, Chae MK, Lee EJ, Yoon JS. 4-Methylumbelliferone suppresses hyaluronan and adipogenesis in primary cultured orbital fibroblasts from Graves' orbitopathy. *Graefes Arch Clin Exp Ophthalmol*. 2020;258(5):1095-1102.
24. Ren Z, Zhang H, Yu H, Zhu X, Lin J. Roles of four targets in the pathogenesis of graves' orbitopathy. *Heliyon*. 2023;9(9):e19250.
25. Saraswathibhatla A, Indana D, Chaudhuri O. Cell-extracellular matrix mechanotransduction in 3D. *Nat Rev Mol Cell Biol*. 2023;24(7):495-516.
26. Szabó L, Balogh N, Tóth A, *et al*. The mechanosensitive Piezo1 channels contribute to the arterial medial calcification. *Front Physiol*. 2022;13:1037230.
27. Shinge SAU, Zhang D, Din AU, Yu F, Nie Y. Emerging Piezo1 signaling in inflammation and atherosclerosis; a potential therapeutic target. *Int J Biol Sci*. 2022;18(3):923-941.
28. Tanabe Y, Koga M, Saito M, Matsunaga Y, Nakayama K. Inhibition of adipocyte differentiation by mechanical stretching through ERK-mediated downregulation of PPARgamma2. *J Cell Sci*. 2004;117(16):3605-3614.
29. Hossain MG, Iwata T, Mizusawa N, *et al*. Compressive force inhibits adipogenesis through COX-2-mediated down-regulation of PPARgamma2 and C/EBPalpha. *J Biosci Bioeng*. 2010;109(3):297-303.
30. Guo Y, Cheng Y, Li H, Guan H, Xiao H, Li Y. The potential of artemisinins as novel treatment for thyroid eye disease by inhibiting adipogenesis in orbital fibroblasts. *Invest Ophthalmol Vis Sci*. 2023;64(7):28.
31. Shen JX, Couchet M, Dufau J, *et al*. 3D adipose tissue culture links the organotypic microenvironment to improved adipogenesis. *Adv Sci (Weinh)*. 2021;8(16):e2100106.
32. Dupont S, Morsut L, Aragona M, *et al*. Role of YAP/TAZ in mechanotransduction. *Nature*. 2011;474(7350):179-183.
33. Zhong G, Su S, Li J, *et al*. Activation of Piezo1 promotes osteogenic differentiation of aortic valve interstitial cell through YAP-dependent glutaminolysis. *Sci Adv*. 2023;9(22):eadg0478.
34. Yang Y, Wang D, Zhang C, *et al*. Piezo1 mediates endothelial atherogenic inflammatory responses via regulation of YAP/TAZ activation. *Hum Cell*. 2022;35(1):51-62.
35. Fu C, Chin-Young B, Park G, Guzmán-Seda M, Laudier D, Han WM. WNT7A suppresses adipogenesis of skeletal muscle mesenchymal stem cells and fatty infiltration through the alternative Wnt-Rho-YAP/TAZ signaling axis. *Stem Cell Reports*. 2023;18(4):999-1014.
36. Wang N, Li Y, Li Z, *et al*. IRS-1 targets TAZ to inhibit adipogenesis of rat bone marrow mesenchymal stem cells through PI3K-Akt and MEK-ERK pathways. *Eur J Pharmacol*. 2019;849:11-21.
37. Ko J, Kim YJ, Choi SH, Lee CS, Yoon JS. Yes-associated protein mediates the transition from inflammation to fibrosis in Graves' orbitopathy. *Thyroid*. 2023;33(12):1465-1475.
38. De Felice D, Alaimo A. Mechanosensitive piezo channels in cancer: focus on altered calcium signaling in cancer cells and in tumor progression. *Cancers (Basel)*. 2020;12(7):1780.
39. Jensen B, Farach-Carson MC, Kenaley E, Akanbi KA. High extracellular calcium attenuates adipogenesis in 3T3-L1 preadipocytes. *Exp Cell Res*. 2004;301(2):280-292.
40. Neal JW, Clipstone NA. Calcineurin mediates the calcium-dependent inhibition of adipocyte differentiation in 3T3-L1 cells. *J Biol Chem*. 2002;277(51):49776-49781.
41. Kim YJ, Hwang SJ, Bae YC, Jung JS. MiR-21 regulates adipogenic differentiation through the modulation of TGF-beta signaling in mesenchymal stem cells derived from human adipose tissue. *Stem Cells*. 2009;27(12):3093-3102.
42. Christodoulides C, Lagathu C, Sethi JK, Vidal-Puig A. Adipogenesis and WNT signalling. *Trends Endocrinol Metab*. 2009;20(1):16-24.
43. Li YM, Xu C, Sun B, Zhong FJ, Cao M, Yang LY. Piezo1 promoted hepatocellular carcinoma progression and EMT through activating TGF-β signaling by recruiting Rab5c. *Cancer Cell Int*. 2022;22(1):162.
44. Miyazaki A, Sugimoto A, Yoshizaki K, *et al*. Coordination of WNT signaling and ciliogenesis during odontogenesis by piezo type mechanosensitive ion channel component 1. *Sci Rep*. 2019;9(1):14762.